Approach to Validate ISPM-15 Compliance for Commercial Treatment Certification of Dielectric Standard Heating of Bulk Solid Wood Packing Materials using Radio Frequency

Karolina K. Szymona John J. Janowiak Ron Mack Mark Hamelin
Mark Gagnon Kelli Hoover

Abstract

To substantially reduce the risk of alien invasive species moving to new geographic areas, phytosanitary treatment of wood packaging materials (WPM) in compliance with the International Standard of Phytosanitary Measures No. 15 (ISPM-15) is required by trading partners. Approved treatments include conventional heating, methyl bromide and sulfuryl fluoride fumigation, and dielectric heating (DH). The DH standard was officially adopted in 2013 but has not been practiced commercially due primarily to insufficient operational validation at commercial scale. In 2022, we converted our 50-kW radio frequency (RF) unit with a 1,200-board foot capacity from an oscillator electromagnetic field power generator to a solid-state power supply, which allows for selective power input adjustments during treatment; we also switched from a five-plate to a three-plate winged electrode system to improve heating uniformity. Each loading cycle can treat sufficient material to build ~94 standard Grocery Manufacturers Association pallets. Our research team characterized the dielectric heating pattern and options for monitoring wood temperatures over a wide-ranging test matrix of WPM that varied by wood species, dimension, moisture content, and loading configuration. We found that this upgraded RF system markedly reduced treatment times and improved heating uniformity, allowing us to develop methods that can be used to verify compliance with ISPM-15 for improved technology transfer to industry. We also discuss the operational cost of RF treatment and make general cost comparisons to conventional heat treatment for WPM.

Invasive species are one of the major causes of global ecological and economic impacts on importing countries through inadvertent introduction during international trade (Olson 2006). In the United States alone, invasive arthropods are estimated to cost the US economy US$54 billion per year, US$2.1 billion of which is damage attributed to arthropod pests of forests (Pimentel et al. 2005). Wood packaging materials (WPM) are a well-known pathway whereby alien pests of forest trees can be introduced into new regions, yet these materials are essential for domestic and global trade. Wood pallets consist of about 90 percent (Digvijay and Onkar 2022) of the worldwide pallet market; they can be repaired, recycled, or reclaimed. The use of wood for making pallets is more environmentally sustainable than the use of plastic (Weththasinghe et al. 2022), and wood pallets have fewer environmental impacts (Kočí 2019). However, if used for export, they must be treated to comply with the International Standard of Phytosanitary

The authors are, respectively, Postdoctoral Researcher, Dept. of Entomology (kss29@psu.edu), Emeritus Professor, Dept. of Agric. and Biological Engineering (jjj2@psu.edu), Penn State Univ., University Park, Pennsylvania 16802; Commodity Treatment Specialist, US Dept. of Agric. Animal and Plant Health Inspection Service, Plant Protection and Quarantine, Science and Technology, Forest Pest Methods Laboratory, Buzzards Bay, Massachusetts 02542 (ron.mack@usda.gov); Chief Operating Officer, RF Kiln Tech Limited, Midland, Ontario, Canada (mark@rfkilntech.com); Associate Teaching Professor, Dept. of Agric. Economics, Sociology and Education (mag199@psu.edu); and Professor, Dept. of Entomology (kxh25@psu.edu [corresponding author]), Penn State Univ., University Park, Pennsylvania 16802. This paper was received for publication in June 2024. Article no. 24-00033.

Forest Prod. J. 74(4):318–330.
doi:10.13073/FPJ-D-24-00033

Measures No. 15 (ISPM-15; Food and Agriculture Organization of the United Nations [FAO] 2013). This standard was established by the International Plant Protection Convention (IPPC) to substantially reduce the risk of alien species in or on wood packaging from moving to new ecosystems. Species introduced into new geographic areas might spread uncontrollably and cause damage to native species. More than 450 forest insect and pathogen species have established in the contiguous United States, and it is estimated that 41.1 percent of the total live forest biomass is at risk of future loss from the 15 most damaging nonnative forest pests (Fei et al. 2019). It is extremely important to prevent these occurrences, and treatments in compliance with ISPM-15 of WPM form one measure that helps to achieve this goal.

Typically, treatment of WPM is accomplished by convection heating in conventional heated air kilns or fumigation with methyl bromide or sulfuryl fluoride. Methyl bromide is environmentally problematic, thus there are strong efforts to phase it out and replace it with other approved phytosanitation methods (United Nations Environment Programme [UNEP] 2000). In 2013, the Commission on Phytosanitary Measures of the IPPC added dielectric heating (DH) as an acceptable treatment method in Appendix 1 to ISPM-15 (FAO 2013). DH can include treatments using microwaves, radio waves (referred to as radio frequency or RF), or ohmic-related heating. DH methods can provide a more rapid approach to effectively sanitize wood packaging (Nelson 1967), and as a DH treatment, microwaves have a more limited volumetric depth of penetration compared to RF (Dubey et al. 2016); therefore, we focused on RF to design a process that can be applied to batch loads of wood material, effectively treating large volumes of prepallet components at one time. To comply with the ISPM-15 standard, the schedule requires heating to 60°C through the profile of the wood load for 1 minute. RF units are not required to be preheated and do not lose a significant amount of energy while heating air, which occurs with conventional heating technology. With RF heating, elevation in ambient air temperature within the treatment chamber is a direct result of heating the wood, since air is not an agent that conducts heat to the WPM. This fundamental difference in the heating process allows for substantial energy savings. Energy efficiency for an RF heating unit can be as high as 95 percent, while for conventional kilns energy efficiency was estimated at approximately 10 percent (Mermelstein 1997, Laborelec 2011).

While DH treatments have been shown to be effective for eradication of pests in WPM (Fleming et al. 2004, 2005; Tubajika et al. 2007; Hoover et al. 2010; Uzunovic et al. 2013; Henin et al. 2014), DH equipment certification protocols have yet to be established in the 10 years since these methods were approved for ISPM-15 treatment. During the preliminary stages of our research to develop a certification protocol for RF, we encountered some operational challenges that negatively impacted heating uniformity. We modified our approach and methodology accordingly as these issues arose, which led to a wealth of practical knowledge about RF technology for treating WPM in compliance with ISPM-15. These experiences were of great benefit in helping shape our testing process in coordination with certification officials, with the ultimate goal of developing a protocol for RF facility certification for bulk treatment of WPM in North America.

To this end, our research team conducted a series of experiments using softwood and hardwood materials while testing several temperature monitoring systems. This included data collection of temperature, treatment time, and power consumption during the RF volumetric heating process. The main objective of this paper is to provide insight into our efforts to optimize RF heat treatment technology for North American certification, and the methods that we used to verify compliance with ISPM-15.

Materials and Methods

Wood material

We performed experiments using freshly sawn green wood material from species that are commonly used in the wood packaging materials industry across North America. The hardwoods red oak (*Quercus rubra)* and yellow poplar (*Liriodendron tulipifera)*, and the softwood white pine (*Pinus strobus*) were tested in single species loads. We also ran tests containing mixed wood species materials, which included red oak mixed with yellow poplar, and red pine (*Pinus resinosa*) and white pine mixtures. Material was custom sawn into full-length dunnage (∼51 by 102 by 2,464 mm [2 in by 4 in by 8 ft 1 in]) and cut-to-length pallet stringers (∼ 25 by 89 by 1,219 mm [1 by 3.5 by 48 in]), which are typically used to construct standard Grocery Manufacturers Association (GMA) pallets. Stringer materials had slightly different widths and thicknesses in one of our experiments (∼29 by 84 by 1,219 mm [1 1/8 by 3 5/16 by 48 in) due to sawing variability in the delivered wood supply from the different lumber mill suppliers. In one experiment, the wood material was fully or partially frozen (red/white pine stringers, Trial 1). In this case, we ran a low power (5 kW/15 min and 10 kW/10 min) thawing cycle followed by a 10-minute rest period with the power off to unfreeze any ice buildup between and within the wood material, thus raising temperatures above 0°C. This thawing cycle was not included in the treatment time for estimating electrical power consumption and calculating treatment cost of heating stringers in compliance with the ISPM-15 dielectric standard.

Experimental RF unit design modifications

The first prototype of our semicommercial scale RF unit (RF Kiln Tech, 6.78 MHz, 50-kW maximum power output) was installed at the Forest Products Laboratory, Penn State University in October 2017. It has a 3-m^3 (1,200 board foot) working volume as the maximum DH treatment chamber capacity, which means that each cycle can treat sufficient component material to build ∼94 standard GMA pallets, representing a pilot commercial-scale operation. The first generation of our RF experimental unit was equipped with a typical five-plate direct current and flat plate electrode applicator system, which divides the workload into four layered sections for RF processing. This older RF prototype is based on self-oscillation circuitry technology for the applied electromagnetic field (emf) frequency, and the electrical power input requires manual adjustment of connections between the variable kilovoltage tap settings. After a series of preliminary experiments, we made several operational

modifications to decrease treatment time and improve heating uniformity. Modeling of heating uniformity by Aethera Technologies (Debaie 2020) suggested that using a three-plate system with a modified middle electrode that featured a wing-shaped attachment would provide improved heating dynamics compared to the five-plate system. Therefore, the middle electrode of our RF prototype unit was modified by attaching an angled flange with a 2.54-mm (1-in)–diameter tube inserted lengthwise on the ends (Fig. 1). The wings are attached to two opposite (longer) sides of the electrode plate. The winged central plate (active) electrode has the first flange element positioned upward toward the top ground plate electrode and a second flange downward toward the bottom ground plate electrode, forming a "wing." The angle formed between the plane of the central plate and each flange is 55°.

At the time we adopted the three-plate winged electrode, our prototype unit was also converted from oscillator emf power generation to solid state (rectified frequency emf operation), which includes an updated matching network (selective treatment cycle RF for power input adjustments). This more advanced technology with solid state circuitry can increase effective power delivery to the workload (95% energy efficiency according to the manufacturer, coauthor M. H., RF Kiln Tech Limited, Ontario, Canada), and was used in our experiments reported herein.

The unit is equipped with a single tuning coil, vacuum capacitors, and glycol liquid cooling system. The human-machine interface (HMI) displays temperature measured with two fiber-optic sensors. The heating rate of the workload can be manipulated by adjusting the selective power input. During experimentation, additional thermal sensors were also utilized to further track thermal developments within the RF volumetric workload (see below).

Wood bulk volumetric configuration for DH treatment

Wood materials were loaded on the RF feed cart in two sections (top and bottom) divided by the middle-winged electrode (Fig. 1). First, we ran replicated dunnage tests, layered nine pieces high in each section and seven pieces across, for a total of 126 pieces (Table 1). Cut-to-length stringer material was also assembled in two front and two back packs relative to the loading door opening. To assess how distribution of the workload affected heating uniformity, the first red oak stringer test was run with material layered in an equal number of pieces in both sections, 15 in the top and 15 in the bottom section (420 wood pieces). For the remaining experiments we modified the loading method, placing 16 layers of stringers in the top section and 14 layers in the bottom section, again with 420 pieces in total. This rebalancing strategy of unequal layering for bulk volumetric configuration of the workload was accomplished to better accommodate the applied power density and help compensate for heat flux (Fig. 2). The dimensions of the load in the chamber, and in particular the height where the driver plate (winged electrode) is located with respect to the centerline of the kiln, drives the balance in heating. In our case, the kiln was never filled to the top, so the applicator sat below the centerline of the kiln. In this position the reflective energy was less on the top, so we expected this area to heat faster. Since the overall pack height was standard in our experiments, we chose to increase the effective power density in the bottom pack by adding it to the top as a single layer addition. Removal of a single layer increased power density to the bottom pack by 12.5 percent. Adjusting the pack depth also increased the RF electrical field intensity as E = V/d, with E = electric field strength and V/d = voltage divided by the distance over which the charge moves between the electrodes. Shortening the distance produces a greater field intensity for a given voltage. This simple modification was enough to significantly improve the overall balance of heating in the load.

Figure 1.—Stringer load with three-plate, middle-wing electrode system with installed fiber-optic temperature probes ready to be loaded into the radio frequency-chamber.

For Trial 3 on red/white pine (Table 1), the top section was assembled with ∼3-mm-thick stickers layered between subsections of five, three, five, and three (16 in total) layers of stringers (Table 1). For Trial 4 on red/white pine, we used the same procedure with ∼13-mm-thick stickers. Care was taken to position the material at an equal distance from the edges of the working table. Under the bottom electrode and on top of the top electrode, we placed a closed-cell, moisture-resistant, rigid foam board (Foamular, R-10, 2-in thickness), to provide additional insulation of the wood material for improved heat retention. Our recent study showed that the application of an insulation layer (or a conduction heat dissipation barrier) can improve the RF heating process for wood materials by reducing evaporative cooling from the wood surfaces (Janowiak et al. 2022). Filler dunnage wood was used to fill the gap between the top load surface and the hydraulic press system, which compresses the load and minimizes possible air gaps. We recorded the total weight of the material utilizing the built-in weighing scale located on the kiln rail. After installing our temperature monitoring systems, we rolled the table into the chamber and secured the chamber door.

Power input adjustment during DH treatment

The power setting was selected on the screen monitor of the RF unit control panel and adjusted in real time, as needed, based on the heating response. We used a 5- to 18-kW power output in the first 5 to 10 minutes of treatment for a "soft start," then increased the power to 35 kW. While testing frozen wood material (red/white pine material, Trial 1;

Table 1.—RF experiments conducted on different wood species cut into stringers or dunnage. Species and average values of power output (P_o), power density (P_d), treated weight (Trt), time when the last fiber optic probe reached 60°C (t_{60}), electrical cost per pallet. Eastern white pine dunnage had dimensions of ~51 by 102 by 2,464 mm (2 in by in 4 by 8 ft 1 in), and stringers ~25 by 89 by 1,219 mm (1 by 3.5 by 48 in), unless indicated otherwise. The number of dots shown after the wood species name indicates the number of trials conducted. All stringers were stacked with 16 layers on the top and 14 layers on the bottom sections, except eastern white pine dunnage, which was stacked nine layers each in the top and bottom sections.

Species	P_o, kW (SEM)	P_d, W/m^3 (SEM)	Trt wt, lb (SEM)	t_{60}, min (SEM)	Electrical cost/pallet, cents (SEM)	Remarks
Yellow poplar/red oak stringers	31.2 (0.13)	19.4 (0.10)	2,109.8	130 (25)	10.9	
Red/white pine stringers[a] ••••	33.1 (0.33)	28.7 (0.29)	1,779.1	90 (9)	11.2	Trial 1[b] – used partially frozen wood, no stickers Trial 2: no stickers used Trial 3: used 3-mm stickers Trial 4: used 13-mm stickers
Yellow poplar stringers •••	30.3 (1.3)	26.2 (1.15)	1,912.5	79 (11)	8.94	
Yellow poplar stringers, 1-1/16 × 3-5/16 × 48 in•	33.3	28.60	1,873.9	66	8.15	
Red oak stringers •••	32.4 (0.64)	28.0 (0.56)	2,850.6	63 (2)	7.62	
Average for stringers	32.1 (0.50)	26.2 (0.43)	2,326.6	86 (6)	9.36	
Eastern white pine dunnage •••	31.2 (0.17)	19.4 (0.10)	2,142.1	147 (9)	13.9	Top and bottom sections assembled with nine layers of dunnage material

[a] While the four trials on red/white stringers were not conducted exactly the same way, we provided the mean and SEM to represent responses in general with this wood mixture; because these trials were not replicated, these data for red/white pine stringers were not used in subsequent statistical analyses.
[b] The time required to thaw frozen red/white pine stringers in Trial 1 was not included in the treatment time (t_{60}).

Table 1), we used the bottom power setting for a prolonged time (~ 30 min) to ensure the material was defrosted before adjusting the kilowatt power to a higher setting as described above. The time and power calculations for thawing wood in a preheating cycle was not included in the treatment time and power consumption calculations for that experiment.

The average power output used for all stringer tests was 32.1 ± 0.50 kW and the average power density was 26.2 ± 0.43 kW/m^3 (Table 1). Using this power adjustment sequence, we were able to maintain consistent (±0.2 kW) RF power input (70% RF emf power generation) for the treatment cycle from start to finish.

Workload temperature monitoring to evaluate ISPM-15 DH schedule compliance (60°C/1 min)

We used and tested several nonconductive temperature monitoring solutions that are designed for compatibility with emfs. Fiber-optic temperature sensors (Oriental RayZer, GF-PU-HP-8m, polyurethane coating) were installed in wood samples in midlength, midwidth drilled holes in 11 locations in dunnage trials (Fig. S1), and in 10 locations for stringers trials (Fig. S2). To prevent probes from becoming dislodged, we secured the sensor leads to the winged electrode using mastic adhesive tape. Probes not properly seated into their wood insertion holes sometimes resulted in erroneous temperature readings. Ten probes were connected to two compatible six-channel data acquisition modules (Oriental RayZer FTM-6CH-H220). Real-time temperature responses were displayed on the data acquisition computer using Oriental RayZer software. Logged data were stored for further analysis. The average final temperature and heating rates were calculated for each run. We performed 2-way analysis of variance (ANOVA) for all replicated stringer wood species combined using location and wood species as the independent variables in JMP Pro (v.16, SAS) to compare the mean top versus bottom temperatures. Before running the analyses, the mean top and the mean bottom temperatures for each trial were calculated and used in the analyses to avoid pseudoreplication. White pine dunnage top and bottom temperatures were compared using 1-way ANOVA separately from stringers.

Disposable, pop-up temperature devices (abbreviated PODs by the manufacturer; Volk Enterprises Inc., L145; 48-mm length) were installed in each wood sample in midlength and midwidth drilled holes (Fig. 3A). PODs are inexpensive, and as single-use thermal indicators, are rated for deploying at 59°C (yellow-coded), 63°C (orange-coded), 71°C (green-coded), 74°C (blue-coded) and 82°C (red-coded); they are manufactured at two lengths: L = 1.825 inches (48 mm) and a shorter version, S = 1.125 inches (29 mm). These devices are made of a durable plastic outer housing body (~3.2-mm inserted housing diameter), and fitted with their respective color-coded deployable plunger, a mechanical compression spring, and a calibrated thermosensitive metal that restrains the outward plunger release (Fig. 3B). After reaching the manufacturer-designed temperature, the metal melts, triggering the plunger to deploy by action of the compressed spring. We utilized the orange type that is designed to trigger when heated to 62.8°C (145°F ± 2°F sensitivity and 1.75-inch (4.45-cm) insertion length, which corresponds to wood material(s) core depth). As their primary use is intended to ensure the cooked temperature of meat in conventional ovens, we tested the thermal indicators for their accuracy in four wood species (eastern white pine [*Pinus strobus*], black cherry [*Prunus serotina*], red oak [*Quercus* spp.], and hard maple [*Acer* spp.]) having moisture content ranging from 10 to 28.1 percent using a forced-air convection oven (VWR Model 1370FM ± 0.5°C heat control capacity). We verified POD triggering temperatures (Table 2) compared to fiber-optic probe installations while strictly monitoring oven temperature settings.

Based on those results, we used PODs as a visual confirmation of the ISPM-15 schedule of ≥60°C in the wood samples throughout the entire bulk volume of the workload

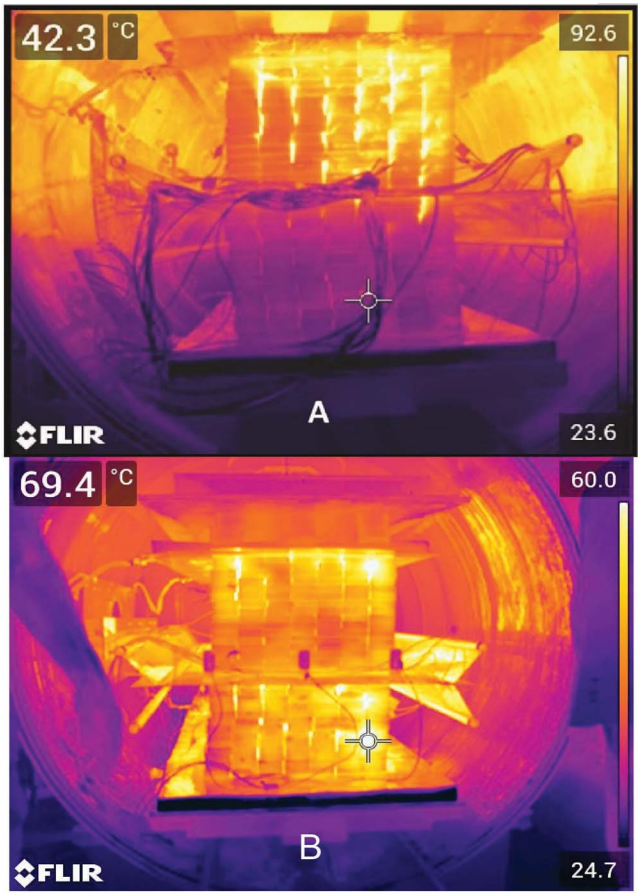

Figure 2.—Example of FLIR thermal images of a wood load after treatment. Images were taken approximately 10 minutes after shutting off the power. Lag time was caused by the process of cooling off the unit before opening the chamber door and unloading the material, (A) red oak stringers (15/15 number of layers in top/bottom sections), (B) red oak stringers inTrial 3 (16/14 number of layers in top/bottom sections). Temperature disparity in (A) the evenly matched load was clearly improved through rebalancing (B) the treated load.

(Fig. 3). We could observe all the PODs installed in the wood samples located in the top section on one side of the load through the viewing port (window) that was housed in the loading door of the RF treatment chamber. The remaining PODs on the opposite side of the load were examined after the treated material was trolleyed outside of the chamber. In a few cases, we identified some PODs that did not deploy; however, the target temperature was still exceeded, which was verified using a manual thermometer (Omega HH147U). If the hole for the POD was not drilled straight, then POD installations required more force to drive the device into the hole with a hammer, which in some cases damaged the device. To avoid this in the future, we found that care is needed to drill the holes straight, with the use of a proper dimension wood-boring bit as opposed to a twist steel type of hole-drilling bit and guiding attachment gear.

Ambient air temperature inside the RF unit chamber was measured to determine if it could be used as a viable indicator of completion of the ISPM-15 dielectric treatment schedule. We used two to four fiber-optic probes (Rugged Monitoring, FOS-TG-06-U-05-C00 with TFFT-014) connected with a four-channel data acquisition system (Rugged

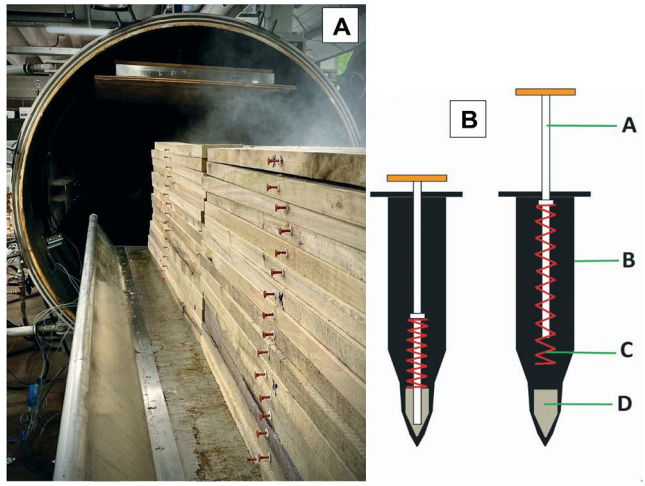

Figure 3.—(A) Pop-up devices (PODs) inserted in stringer material, visibly deployed, which indicated minimum temperature of 62.8 °C. (B) Scheme of POD components; A -plastic stick, B — outer case, C — spring, D — soft metal; left image represents POD designed with the working temperature threshold of 62.8 °C, right image shows deployed POD.

Monitoring, T301-04-E1A0R8M4). Rugged Connect software was used to track thermal development and data logging of varying air temperature in locations inside the RF chamber during the treatment process.

After the treatment was completed and the load was removed from the chamber, we captured thermal images of the load with an infrared (IR) imaging camera (FLIR, Model 530), which provided wood surface temperatures (example in Fig. 2B). The IR images were taken after a 10- to 15-minute delay, which is the time required to shut down RF power, open the pressure sealed cylinder door, and roll the wood load out of the treatment chamber. Thermographic images were taken after each completed test to evaluate both the end grain and sides of the heated workload to document wood surface heating patterns for DH compliance.

For Trial 4 on red/white pine stringers, we collected the core temperature of 60 samples with a manual temperature meter (Omega, HH147U). Collection of thermal readings was conducted within 20 minutes (plus 8 min for unloading) to avoid temperature measurement bias from surface cooling of the wood material following the completed RF heating trial. The readings were directly collected at the POD locations, with indicators extracted immediately before the meter probe measurement to avoid water vapor heat release.

Table 2.—Heating responses of orange coded pop-up temperature devices in wood samples heated in a conventional convection laboratory oven.

Species	MC, %[a]	P_1, °C	P_2, °C	T_p, °C	ΔT, °C
Eastern white pine (*Pinus strobus*)	10	64.5	63.4	64.0	1.2
Black cherry (*Prunus serotina*)	5.2	65.0	66.8	65.9	3.1
Red oak (*Quercus* spp.)	28.1	65.1	65.9	65.5	2.7
Hard maple (*Acer* spp.)	15.6	65.2	66.6	65.9	3.1
Average	14.7	65.0	65.7	65.3	2.5

[a] MC = Average moisture content; P_1 = trigger temperature for first pin; P_2 = trigger temperature for second pin; T_p = average trigger temperature; ΔT = difference between observed and designed triggering temperature.

After collecting the 60 temperature readings for the entire outer side of the heated pack quadrants, we calculated the corresponding average temperature and standard error for the four quadrants and compared these values to the overall population average and standard error. We then determined the number of PODs that should be installed in a load for treatment verification at a high degree of confidence during the certification process, utilizing the formula from Huntsberger and Billingsley (1987) for the sample size required based on the standard deviation, to calculate the 95 percent confidence interval (CI): ($Z_{\alpha/2} = 1.96$) and the 99 percent CI: ($Z_{\alpha/2} = 2.576$), respectively; the width of the confidence interval with width (W) = 5.4°F, and SD (standard deviation) = 10.8°F:

$$W = 2 \times Z_{\alpha/2} \times \frac{\mathrm{SD}}{\sqrt{n}}$$

Treatment cost comparison between RF and conventional heating

The cost of RF treatment using our data for electrical power consumption was compared to referenced cost quotes for conventional wood heating kilns that apply heat to wood by directly heating the air. We calculated cost per RF treated pallet using current electrical (kWh) pricing for the annual average (9-mo, 2023) industrial user according to the US Department of Energy (2023; Table 1). Electrical cost for RF treatment is derived as follows:

$$\mathrm{P_0(kW)/P_d(kW/m^3)} \times 423.776\,(\text{board-foot scale})/13.5\,(\text{board feet per pallet}) = \text{treated GMA pallet units;}$$

$$\mathrm{P_0(kW)} \times \mathrm{t_{60}(h)} \times \text{industrial user cost}\,(8.13\text{ cents per kWh})/\text{number treated GMA pallet units} = \text{electrical cost per pallet.}$$

Results and Discussion

Preliminary observations through nonreplicated testing

Prior to completing the replicated experiments reported herein, we performed a series of preliminary experiments over the course of several years with our first-generation, five-plate electrode RF system design. We tested the RF unit's capabilities and limitations during treatment of WPM components. Due to limitations on the ready availability of wood components from 2020 through 2022, labor shortages, and travel restrictions from the impacts of Covid-19, wood components available to us often varied in moisture content, sometimes significantly within a single batch of material, and it was challenging to source particular species or dimensions that we wanted to test within a reasonable timeframe to allow for similar initial temperature and moisture conditions in the wood. During the winter, we often received frozen wood material that needed to be conditioned at room temperature for extensive periods of time, which led to decreasing wood moisture content in parts of the batch. Initial temperatures of wood material greatly affected the duration of treatment in compliance with ISPM-15. The RF treatment process used for frozen wood requires special consideration because the frozen layers do not interact with the electromagnetic field at the same rate as unfrozen material (Rattanadecho 2004). Thus, for one trial (Trial 1) with frozen wood (red/white pine stringers), we found it helpful to use a short thawing cycle with a reduced power setting to elevate the frozen wood temperature up to approximately 0°C before the full power setting was utilized (Table 3). The final average temperature was thus higher in Trial 1 compared with Trial 2, which also had a higher initial temperature after the wood was thawed. Consequently, heating rates were slower in Trial 1 compared with Trial 2 in the top and bottom sections (0.76°C/min ± 0.06°C/min and 0.93°C/min ± 0.01°C/min vs. 0.97°C/min ± 0.06°C/min and 1.12°C/min ± 0.07°C/min, respectively). This translated to a longer treatment time, which was 102 minutes for the load with initially frozen material (Trial 1), and only 63 minutes for nonfrozen material (Trial 2; Table 4). Even though controlled conditions for every experiment were difficult to achieve, this will often be encountered in real-world commercial treatment, but operational flexibility of the RF system will successfully handle this variability.

While we could not always replicate some experiments due to limitations in wood material availability, our preliminary experiments allowed us to come to a better understanding of the RF process and informed the direction we took in our research and subsequent modifications of the technical components of the equipment. For example, our experience treating stringers rather than cants allowed us to stack the load tighter with fewer air gaps, which improves conductive heat exchange, heating uniformity, and heating rate. We also examined the possibility of treating wood components that are assembled in a pack with bundling stickers to simulate a routine industrial practice. Thus, unreplicated Trials 3 and 4 with a mix of red and white pine stringers were performed with 3- and 13-mm stickers, respectively, which created air gaps in the load, and potential disruption of the heating process. For comparison purposes, stickers were only used in the top section of the material. In the 3-mm stickered trial, the top section reached a final temperature of 91.4°C ± 8.1°C compared with 103.6°C ± 2.3°C in the bottom section without stickers (Table 3). Similarly, the heating rate was 0.81°C/min ± 0.08°C/min in the top section of 3-mm stickered material, while it was 0.96°C/min ± 0.02°C/min in the material in the bottom section without stickers. In the experiment with thicker 13-mm stickers in the top section, the

Table 3.—Final temperatures and heating rates for bottom versus top sections of the load for radio frequency treatment of red/white pine stringers.

Trial	Remarks	T_t, °C (SEM)[a]	T_b, °C (SEM)	HR_t, °C/min (SEM)	HR_b, °C/min (SEM)
1	Frozen material, no stickers used	82.0 (6.6)	103.3 (2.6)	0.76 (0.06)	0.93 (0.01)
2	No stickers used	75.5 (6.7)	84.8 (7.2)	0.97 (0.07)	1.12 (0.07)
3	3-mm stickers	91.4 (8.1)	103.6 (2.3)	0.81 (0.08)	0.96 (0.02)
4	13-mm stickers	83.6 (8.9)	108.2 (0.4)	0.78 (0.10)	1.03 (0.01)

[a] T_t = Final temperature of the top section; T_b = final temperature of the bottom section; HR_t = heating rate of the top section; HR_b = heating rate of the bottom section.

Table 4.—Time to complete radio frequency treatments for each trial and criteria used to terminate treatment. Top to bottom assembly of the load: 9/9 for eastern white pine dunnage, and 16/14 for all stringers.

Species	Trial no.	t_{60}, min[a]	Ta_{60}, °C	t_t, min	Criteria for terminating experiment	POD remarks
Yellow poplar/red oak stringers	1	154	98.6	163	Most visible PODs triggered	3 PODs did not trigger, but posttreatment measurements were >63 °C
	2	105	Nd	105	Last fiber-optic probe read 60°C	All PODs triggered
Red/white pine stringers	1[b]	102	57.3	135	All PODs triggered	All PODs triggered
	2[c]	63	33.3	100	Ambient air = 56°C	All PODs triggered
	3[d]	104	65.4	115	All PODs triggered	All PODs triggered
	4[e]	91	68.5	110	Most PODs triggered	1 POD did not trigger, verified posttreatment as damaged POD
Yellow poplar stringers	1	69	44.6	90	Ambient air = 60°C	All PODs triggered
	2	101	55.2	106	Ambient air = 56°C	All PODs triggered
	3	67	41.9	89	Ambient air = 56°C	All PODs triggered
Yellow poplar stringers, 1 1/16 × 3 5/16 × 48"	1	66	56.0	78	Ambient air = 56°C	All PODs triggered
Red oak stringers	1	63	36.3	125	Ambient air = 60°C	All PODs triggered
	2	67	36.1	120	Ambient air = 60°C	All PODs triggered
	3	59	36.6	135	Ambient air = 60°C	All PODs triggered
Eastern white pine dunnage	1	164	51.1	164	Wood temp = 60°C	6 PODs did not trigger
	2	143	58.2	143	Wood temp = 60°C	1 POD did not trigger, posttreatment measured 62.4°C
	3	133	41.4	133	Wood temp = 60°C	All PODs triggered

[a] t_{60} = Time when the last fiber optics probe reached 60°C; Ta_{60} = ambient air temperature when all fiber optics probes installed in wood showed ≥ 60°C; t_t = total treatment duration based on when last POD triggered; POD = pop-up temperature device; Nd = not determined.
[b] Partially frozen load and no stickers.
[c] No stickers.
[d] 3-mm stickers.
[e] 13-mm stickers.

difference in heating rate was even more pronounced (0.78°C/min ± 0.1°C/min for stickered and 1.03°C/min ± 0.01°C/min for no stickers). Treatment times were 104 and 91 minutes for the trial with 3- and 13-mm stickers, respectively, which was longer than Trial 2 (no stickers used, 63 min; Table 4). Although the treatment duration increased, treatment was completed successfully. While the stickered material experiments were not replicated, observations indicate that stickers can be present in bundled packs without a need to change RF treatment methodology. This means that material could be kept in banded packs, as prepared by sawmill facilities, which is an added commercial advantage. Handling banded units of material for treatment loading in a three-plate configuration will be much more time efficient than the five-plate arrangement. However, this approach may require banding the material units with non-dielectric conductive straps (e.g., plastic), as opposed to use of metal banding straps.

Upgrade of RF unit from a five-plate to a three-plate winged electrode system

A heating response modeling report that we commissioned using a three-dimensional electrostatic model in COMSOL (Aethera Technologies) suggested that the three-plate system with a middle wing electrode can provide a substantial improvement in the heating process and can achieve heating uniformity that is equal to or better than the five-plate electrode design while using less energy (Fig. 4). The model compares these two designs in the application of a 6.78-MHz RF wave, which we also used in our experimental RF unit, for relative permittivity = 3 and relative permittivity = 10 with the same dissipation factor = 20 percent. These were meant to present the worst-case scenario for uniformity comparison. In both modeled cases, results showed that simply using a three-plate design without modifications would worsen the heating uniformity, but addition of the wing attachment to the center electrode increases heating uniformity by reducing the hot and cold spots in the load. The winged electrode focuses RF on- the center of the wood load, using applied energy more efficiently and decreasing heating variations that occur without the wings attached. This modification can reduce treatment time while saving energy consumption costs. The impedance of the kiln is doubled for a load, which means that the feed current into the kiln is cut in half for the same power input, reducing the thermal stress on the wood. Another advantage of the three-plate winged electrode system over the five-plate system is that it shortens the time of loading the material, because the load needs to be divided into only two sections versus four. The increase in impedance and the associated reduction in RF kiln input current of the three-plate configuration will allow for the application of more power into a wider range of wood species, densities, and moisture contents before the limits of the matching network components are reached.

Our preliminary, unreplicated experiments on yellow poplar performed using the older five-plate design took 104 minutes to complete, while replicated results produced with the three-plate unit with winged electrode had shorter heating times for poplar of 79 ± 11 (SEM) minutes on average (Table 1). Similarly, we noted significant improvement for pine wood; the older unit took 163 minutes to complete the treatment while using the new design system required 90 ± 9 minutes on average for treatment, which is 45 percent faster. IR images taken after the material was unloaded showed that the load heated more uniformly, which confirmed the advantages of using the three-plate, winged-electrode design.

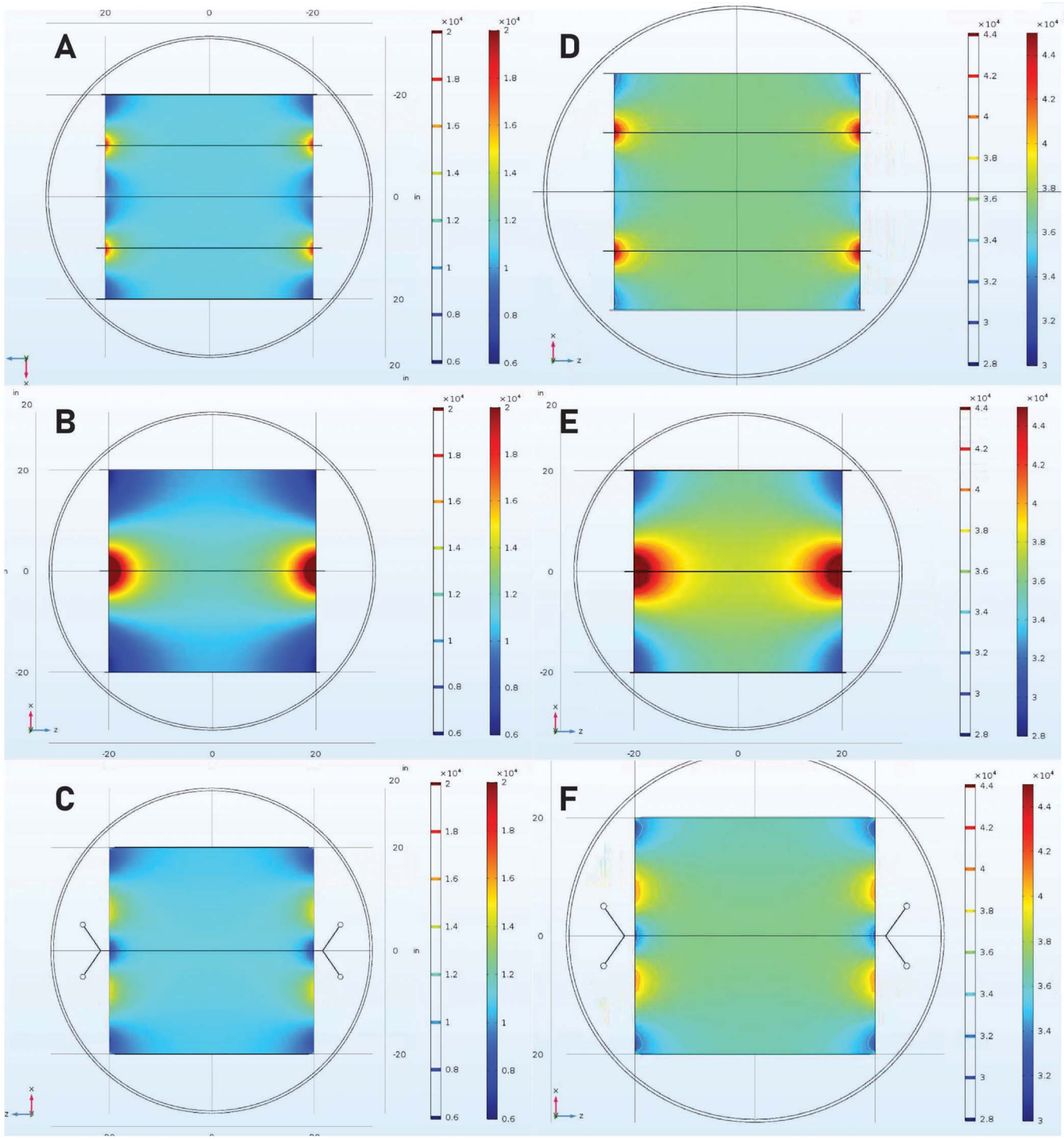

Figure 4.—Models prepared by Aethera Technologies using a three-dimensional electrostatic model in COMSOL and dissipation factor = 20%. (A, B, C) Relative permittivity = 3; (D, E, F) relative permittivity = 10. (A and D) temperature distribution using the five-plate electrode system, (B and E) temperature distribution using three-plate system with flat electrode, (C and F) temperature distribution while using three plates with winged middle electrode. Temperature distribution worsens if three-plate system with conventional, flat electrode is used, developing bigger hot and cold spots. However, adding wings to the middle electrode in the three-plate system greatly improved heating distribution throughout the load.

Temperature monitoring to confirm compliance with the ISPM-15 DH schedule

While testing different types of wood material, our focus was simultaneously directed toward examining temperature monitoring and verification systems. Appendix 2 of the Draft Guidelines for the Application and Verification of Dielectric Heating describes the use of fiber-optic sensors, nonconductive thermocouples, and IR cameras to verify achievement of the DH schedule (60°C through the workload for 1 min; International Forestry Quarantine Research Group 2012). We realized that the characterization of electromagnetic conditions in the RF chamber would require a

robust temperature monitoring system that is compatible with high temperatures and excessive moisture and can similarly withstand the corrosive properties produced by the wood inside the sealed chamber.

Early experiments demonstrated that fiber-optic probes were prone to costly breakages with sometimes faulty temperature readings during treatment. Switching to a more robust fiber-optic probe through a different manufacturer largely solved that problem. Additionally, temperature monitoring systems for industrial RF heat treatment of wood in compliance with ISPM-15 must be economically and operationally efficient and easy to maintain. To that end, we leveraged the observation that the edges of the exposed outer wood surfaces tend to be cooler due to evaporative cooling (Dubey et al. 2016, Janowiak et al. 2022), therefore, temperature monitoring on the sides of the workload can provide sufficient confirmation of completion of the heating process. With this in mind, we examined several temperature monitoring solutions that could be applied during RF sanitation treatment of WPM.

During preliminary experiments, we tested a thermal camera with an automatic spot-finder installed on the inner chamber wall for real-time thermal imaging of the load (Optris Xi 400 IR, −20°C to 900°C). Due to the close distance of the lens and its operating angle, it provided limited information on the temperature of the overall wood load. Additionally, we noticed that the lens of the camera tended to fog up as air humidity conditions increased inside the chamber, making it difficult to measure temperature of the wood surface.

We utilized a FLIR imaging camera for taking thermal readings of the sides of the load after unloading the wood from the RF unit (Fig. 2), but this use has its limitations. There is a time delay before images can be taken as the operator turns off the unit, opens the door, and unloads the wood material, which takes ∼8 to 10 minutes in total. Although we took images as soon as possible, the cooler ambient air temperature was causing rapid heat dissipation as it contacted the wood surface, which was especially apparent in cooler winter months when we had the overhead doors open in the work area to vent steam posttreatment. The IR images only show the temperature on the wood surface, thus rapid surface heat dissipation causes reduced accuracy of peak temperature readings than were present before removing the wood from the RF chamber. While this method can be used as a convenient visual confirmation of heating uniformity, it is not advisable to use it as the only confirmation method following treatment. However, we did find it useful to identify colder sections of wood materials, which were then followed by manual temperature readings in those locations.

While IR images could be taken only after completion of the treatment and removal from the chamber, fiber-optic temperature sensors installed in wood samples proved to be useful in delivering real-time temperature data, allowing for monitoring of the entire process. Temperatures were displayed on the computer screen and plotted over time, providing information about heating rates (example of a typical heating response is presented in Fig. 5). However, fiber-optic sensors also have some limitations. The sensors need to be securely installed in a sample so they will not slide out of the drilled holes when temperatures are increasing, causing the wood to release hot steam. False low readings can

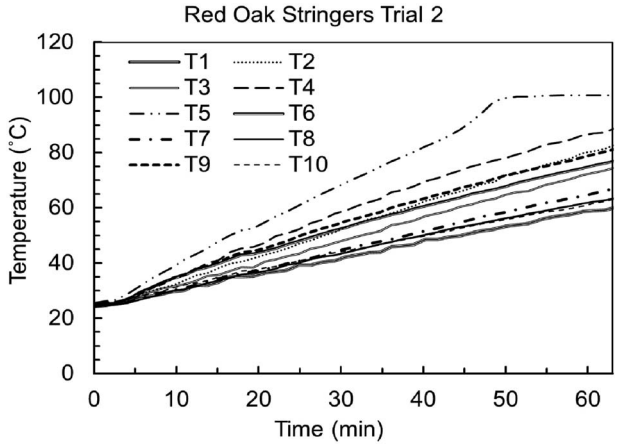

Figure 5.—Example of temperature plot based on fiber optic temperature readings during red oak stringers (Trial 2) radio frequencey experiment.

potentially prolong the treating cycle, resulting in overheating of parts of the load. Frequent use in wood causes probes to wear out over time; their protective coat starts to strip off and expose the fragile sensor, which becomes damaged. The probes are relatively expensive to replace, adding to the cost of operation of the unit. There is also a limitation on how many probes can be used at one time; increasing their number increases the time required to prepare the workload and creates a "web of cables," which tend to tangle.

Due to these issues, we investigated the possibility of using the chamber's "ambient" inside air temperature to determine when to terminate treatment, which would represent a hassle-free monitoring system (see Table 4). Unfortunately, the ambient temperature for yellow poplar/red oak stringers used in Trial 1 was unusually high, and for other species, it showed a lot of variability, e.g., ranging from 33.3°C to 68.5°C in red/white pine experiments, which indicates that air temperature in the unit is not a reliable predictor of RF treatment time.

Thus, we tested disposable PODs as a potential treatment verification method for industrial DH application in wood by first assessing their accuracy and reliability in a conventional oven. On average, each yellow and orange POD triggered ∼2.5°C above the rated indicator performance (Szymona et al. 2020; Table 2). None of the orange PODs that are supposed to trigger at 62.8°C performed below the designed temperature threshold as stipulated by the manufacturer, with the lowest reading of a triggered POD at 63.4°C. We found that the PODs provide a 4.7 percent safety margin (triggering at 62.8°C, which is 2.8°C higher than the 60°C requirement) for proper compliance with the ISPM-15 dielectric schedule.

Table 4 presents summary results on the treatment time when the last fiber-optic probe reached 60°C or all PODs deployed for each wood species and dimension, the total duration of the experiment, and the criteria for terminating the experiment (turning off the power). Calculations presented in Tables 1 and 3 through 7 are based on the last fiber-optic probe reaching 60°C to turn off the RF unit. For eastern white pine dunnage (Trial 1), PODs did not trigger in six locations that were placed in air-exposed (workload edge) pieces. Manual meter checks (25 to 30 min time delay

posttreatment) conducted near the installed PODs indicated that wood temperature was slightly below 60°C. We think these observations were due to the preheat check conducted 12 hours earlier to verify proper functioning of the existing heat exchanger at a higher 40-kW power input calibrated with operational power. This may have caused an alteration of the free water equilibrium within the wood core section sufficient to induce both an RF impendence change and corresponding modification of wood dielectric properties of the outside pieces relative to the inner bulk stack.

We also compared the time required to complete RF treatment in compliance with the ISPM-15 schedule using these two different approaches to temperature monitoring, i.e., the time at which all PODs installed in the load deployed and the time when the last fiber-optics probe reached 60°C for at least 1 minute (Table 4). We found that the last of the PODs to deploy required an average of 125.6 ± 9.7 minutes, while the time for the last fiber-optics probe to reach 60°C was 111.2 ± 10 minutes; thus, treatment time based on the fiber optics was 12 percent faster, which was expected given the slightly higher triggering temperature and large number of PODs we used in this study. Moreover, a regression analysis found that the time in minutes at which all PODs deployed can be predicted from this equation: POD = 32 + 0.84 × fiber optics (linear regression: $F = 12.3$; df = 1,4; $P = 0.0246$).

Table 5 summarizes the results of a 1-way ANOVA comparing the mean posttreatment temperatures at the locations where the PODs were installed for Trial 4 of the red/white pine treated pack quadrants. We found that the wood pieces in the upper sections (Quadrants 1 and 2) yielded statistically significant lower final core temperatures than the bottom (Quadrants 3 and 4) within the RF-heated pack units, but all four quadrants exceeded the required ISPM-15 temperature.

Using the formula in the "Materials and Methods" section above for determining the number of PODs needed to achieve sufficient confidence in the accuracy of the temperature at which the PODs deploy, we found that 61 PODs would be needed to detect a thermal heating range of W = 3°C using a 95 percent CI, and 106 PODs using a 99 percent CI. This level of temperature monitoring would not be considered feasible in an industrial setting but would help support initial qualification of equipment by determining cold spots in the load. RF equipment operational parameters that impact heating uniformity would then be reviewed and discussed between the regulatory agency and the treatment provider to ensure optimal performance. To the extent that heating is deemed sufficiently uniform, a reduction in the number of probes to a more practical number (e.g., four to six per side) would be justified. Final determination of number and placement of temperature monitoring probes and/or PODs will be dependent on the location and consistency of cold spots in the treated load as identified on site by the regulatory agency for a particular piece of RF treating equipment.

Table 5.—Posttreatment average temperature measured by pop-up temperature device locations during the radio frequency red/white pine Trial 4: 1-way ANOVA: F = *13.4; df = 3,56;* P < *0.0001. Averages followed by a different letter are significantly different using Tukey's HSD,* P < *0.05. Location of the four quadrants indicated in Supplemental Figure S2.*

Quadrant	Avg, °C[a]	SEM
1	89.6a	1.4
2	88.8a	1.2
3	97.4b	1.1
4	96.6b	1.1
Total	93.1	0.8

[a] Avg = average temperature in each of the four subsections (quadrants).

Performance of RF across all experiments

The first trials for the study on eastern white pine dunnage were performed using nine layers of wood in each of the top and bottom quadrants; we found that the mean temperature in the top was cooler than the bottom by about 6°C (Table 6). This led us to change the loading method for all experiments, thereafter, placing one more layer of stringers in the top section, while reducing the bottom section by one layer, (i.e., 16 pieces on the top and 14 on the bottom). As a result, we noted that all further experiments using stringers (excluding unreplicated trials for red/white pine in the analysis), revealed no significant difference in the mean temperature in the top compared with the bottom quadrants ($F = 1.41$; df = 1,16; $P = 0.2526$), even when taking wood species into account in the analysis (top: 79.4°C ± 3.79°C and bottom: 85.0°C ± 3.80°C; Table 6). Dunnage stacked nine layers on the top and bottom was analyzed separately from stringers and we found that wood on the top was significantly hotter than the bottom (90.4°C ± 3.32°C and 77.5°C ± 3.32°C; Table 6). These findings suggest that POD installations are less critical for monitoring both the bottom and top sections for stringers, while satisfying the established safety margin within the volumetric batch of RF-treated materials. The average temperature on the right side of the pack (Quadrants 1 and 3) and for the left-side quadrants (2 and 4) were also similar, differing by approximately 7.8°C.

If an RF unit should show heating disparity in heating between the top and bottom pack, this could be resolved with installation of a high electrical voltage-to-power switching control where the applied RF emf is selectively terminated upon reaching 60°C. This operational modification would help minimize unnecessary energy consumption and reduce risk of overheating the workload and would also be favored when loaded packs include a mix of wood species with dissimilar dielectric properties.

Economic efficiency of RF technology

For our experiments treating simulated commercial workloads (1,200–board foot capacity) in the 50-kW RF phytosanitary oven housed at Penn State University, the average electrical consumption cost per pallet for all wood species treated as stringers was calculated as US$0.09 per pallet, and average electrical cost for treated white pine dunnage was US$0.14 per piece (Table 1). Prior study by Szymona and Janowiak (2019) that modeled commercial RF treatment cost based on true power in a leased 6,000–board-foot-capacity RF drying kiln discovered similar and even improved electrical cost numbers at true commercial scale. For comparison, a representative electrical cost analysis of conventionally heated Canadian softwood resulted in a US $0.15 per pallet (S. Geffros, General Manger, Canadian Wood Pallet and Container Association, personal communication, 2023). This conventional heating cost estimate is further corroborated by Gagnon et al. (2019) through a survey of National Wooden Pallet and Container Association manufacturers in the US. The actual cost of conventional

Table 6.—Average values during RF experiments. Stringer trials were assembled with 16/14 layers in the top to bottom section configuration. Eastern white pine dunnage was assembled with 9 layers each on top and bottom. Mean temperatures followed by the same letter are not significantly different at $P < 0.05$. *See Table 7 for ANOVA results.*

Species	T_t, °C (SEM)[a]	T_b, °C (SEM)	HR_t, °C/min (SEM)	HR_b, °C/min (SEM)
Yellow poplar/red oak stringers	73.9 (11.8)a	96.6 (15.9)a	0.55 (0.17)	0.65 (0.00)
Red/white pine stringers[b]	83.1 (3.29)	100.0 (5.2)	0.83 (0.05)	1.01 (0.05)
Yellow poplar stringers	85.0 (1.6)a	85.3 (1.6)a	0.85 (0.09)	0.85 (0.10)
Yellow poplar stringers, 11/16 × 35/16 × 48"	81.2	84.2	0.92	0.95
Red oak stringers	75.8 (2.6)a	77.1 (2.6)a	0.81 (0.02)	0.84 (0.08)
Eastern white pine dunnage	90.4 (3.3)a	77.5 (3.3)b	0.50 (0.03)	0.41 (0.05)
Average	82.2 (2.9)a	83.2 (2.9)a		

[a] T_t = Final temperature of the top section; T_b = final temperature of the bottom section; HR_t = heating rate of the top section; HR_b = heating rate of the bottom section.

[b] Time to defrost frozen wood in Trial 4 red/white pine was not considered in total treatment time. Red/white pine stringers were not included in the ANOVA since the four trials were not conducted in the same way (see Table 1). Eastern white pine dunnage was analyzed separately from stringers.

heating is highly variable, and depends greatly on chamber type, efficiency of chamber insulation and air movement, load orientation, treatment time, and wood species and dimension, among other factors.

These cost calculations demonstrate that RF is economically competitive with conventional heating for the cost per pallet, and in fact has additional economic advantages in overall heating efficiency. Jiao (2012) documented the instant heating capability and efficiency of volumetric DH over conventional heat transfer methods. Even though modern conventional phytosanitary heating equipment has improved in many respects, like higher and more uniform air flow, more uniform temperature distribution, and improved humidification systems since the days of conducting operations in dry kilns, a significant amount of heat is lost by several recognized factors, including air transfer of heat through the equipment structure (Shottafer and Shuler 1974, US Department of Agriculture 1991). Dubey et al. (2016) noted that DH heating of dielectric materials such as wood, which has poor electrical and thermal conduction properties, heats the wood directly without the need to depend on heat transfer from air to the wood, which is far less energy efficient. The authors also mentioned that further evidence of RF efficiency was reflected in the approved phytosanitary treatment schedules in ISPM-15, with RF approved at 60°C for 1 minute, while conventional heating requires maintaining 56°C for 30 minutes throughout the profile of the wood.

The findings reported herein are applicable to this specific piece of RF equipment; each RF unit must be tested to locate potential cold and hot spots and to evaluate the most reliable methods for monitoring temperatures. From our results, the use of PODs with a few fiber-optic probes provide reliable, accurate means of monitoring temperatures to ensure compliance with the ISPM-15 DH schedule and should be able to be used for certification of RF units.

Conclusions

In summary, the average treatment time in our experiments ranged from 63 ± 2 minutes for red oak stringers to 147 ± 9 minutes for eastern white pine dunnage (Table 1), with an overall average of 86 ± 6 minutes for all stringer trials. The average final temperature registered by fiber optic sensors was 86.2°C ± 1.24°C with an average heating rate of 0.75°C/min ± 0.04°C/min and an average moisture loss of 4.4 ± 0.56 percent (Table 7). Coefficient of variation was 8.2 percent on average and lowest for red oak stringers (1.9%; Table 7), indicating low variability in final temperatures. Clearly, use of PODs and several fiber-optic temperature sensors to monitor each load ensured attainment of final temperatures throughout the profile of the wood above the required 60°C for 1 minute.

Extensive experimentation on a range of treatment parameters has demonstrated that bulk RF heating is a viable alternative to the use of conventional kilns for the heat treatment of WPM and should be considered for commercial certification in North America. Wood species testing that we have conducted to date, which included both hardwoods and softwoods, spanned the range of differences in dimension (e.g., cants, stringers, dunnage), density, moisture content, and permittivity that would likely be encountered in commercial applications. RF equipment modification from an oscillator based five-plate system to a solid state three-plate system with winged intermediate electrode helped to significantly improve heating uniformity and overall treatment times. Data gathering and observations on applied power levels, load rebalancing, RF-compatible stickering, and proper application of an insulation layer applied to outer ground plates all provided benefit to overall treatment optimization. To ensure compliance with the DH schedule of ISPM-15, we found that fiber-optic probes, thermal indicator devices (PODs), and thermal imaging produced a thorough and reliable treatment temperature monitoring system that allowed us to calculate the number of PODs required for dielectric treatment validation (60°C for 1 min hold). In commercial practice, the simple utility and low cost of PODs will provide treatment providers with a desirable monitoring solution, and initial steps taken to determine heating uniformity through cold spot mapping and optimized equipment operation will help justify the reduction of the number of PODs required by calculation to a more practical number.

RF treatment schedules are faster and more cost efficient than the traditional methods of heat-treating WPM, and results from commercial RF operations suggest that operating costs are further reduced when the technology is scaled up. An added benefit is that RF treatment does not use chemicals in the process, resulting in a much more environmentally friendly operation. RF has already been adapted to

Table 7.—Average values based on readings of all temperature sensors installed in the wood loads during radio frequency experiments.

Species	T_i, °C (SEM)[a]	T_f, °C (SEM)	CV_{Tf}, %	Ta_{60}, °C (SEM)	HR_w, °C/min (SEM)	HR_a, °C/min (SEM)	ML, % (SEM)
Yellow poplar/red oak stringers	12.4 (0.37)	87.8 (5.33)	7.5	98.6	0.60 (0.08)	0.52	5.1 (4.05)
Red/white pine stringers	10.04 (0.46)	91.55 (5.02)	8.6	56.1 (8.0)	0.82 (0.06)	0.39 (0.07)	6.4 (0.87)
Yellow poplar stringers	21.0 (0.11)	86.0 (4.26)	8.6	49.4 (3.6)	0.85 (0.09)	0.40 (0.10)	3.8 (0.27)
Yellow poplar stringers, 1 1/16 × 3 5/16 × 48 in	20.9 (0.31)	82.7 (4.15)	NA	56.0	0.94	0.71	2.1
Red oak stringers	24.7 (0.15)	76.5 (4.42)	1.9	36.3 (0.1)	0.83 (0.04)	0.15 (0.01)	3.2 (0.38)
Eastern white pine dunnage	18.2 (0.47)	84.5 (5.09)	5.3	50.2 (4.9)	0.46 (0.04)	0.21 (0.03)	5.4 (1.28)
Average	17.4 (0.44)	86.2 (1.24)	8.2	52.6 (3.9)	0.75 (0.04)	0.30 (0.04)	4.4 (0.56)

[a] T_i = Initial temperature of wood material; T_f = final temperature of wood material; CV_{Tf} = coefficient of variation of mean final temperatures; Ta_{60} = ambient air temperature when the last wood temperature probe reached 60°C; HR_w = wood heating rate; HR_a = heating rate of an ambient air temperature; ML = moisture loss; NA = not applicable.

commercial scale for drying operations, making the crossover to this heat treatment technology easier to implement for WPM operations.

Results obtained in this study should position bulk RF treatment of WPM for North American certification and acceptance by industry. Regulatory policy for facility certification will be developed by the certifying agency that outlines initial qualification through demonstration of heating uniformity to the dielectric standard (Step 1), followed by an approved temperature monitoring scheme and RF treatment documentation plan during operation (Step 2).

Acknowledgments

This project was funded by the US Department of Agriculture (USDA) NIFA Methyl Bromide Transitions Grant (Award 2020-51102-32919). We also acknowledge support from USDA Hatch Project Accession number 1021211 and Project Number PEN04728. The American Lumber Standards Committee and Canadian Lumber Standards and Accreditation Board observed experimental trials and provided comments on a draft of this manuscript. The findings and conclusions in this publication are those of the authors and should not be construed to represent any official USDA or US Government determination or policy. This material was made possible, in part, by a cooperative agreement from the USDA's Animal and Plant Health Inspection Service (APHIS). It may not necessarily express APHIS' views.

Literature Cited

Debaie, A. 2020. Heating uniformity with five plates vs three plates in 62″ diameter kiln. Aethera Technologies Limited. Report. Halifax, Nova Scotia, Canada.

Digvijay, P. and S. Onkar. 2022. Pallets market by material (wood, plastic via injection molding, plastic via other methods, corrugated paper, metal), by type (rackable, nestable, stackable, display), by application (rental, non-rental), by end-user (food and beverage, chemical, retail, pharmaceutical, others). Global Opportunity Analysis and Industry Forecast, 2015–2030. https://www.precedenceresearch.com/pallets-market, accessed April 5, 2024.

Dubey, M. K., J. J. Janowiak, R. Mack, P. Elder, and K. Hoover. 2016. Comparative study of radiofrequency and microwave heating for phytosanitary treatment of wood. *Eur. J. Wood Sci.* 74:491–500.

Fei, S., R. S. Morin, C. M. Oswalt, and A. M. Liebhold. 2019. Biomass losses resulting from insect and disease invasions in US forests. *Proc. Natl. Acad. Sci. U. S. A*. 116(35):17371–17376. https://doi.org/10.1073/pnas.1820601116

Fleming, M. R., J. J. Janowiak, J. M. Halbrendt, L. S. Bauer, D. L. Miller, and K. Hoover. 2005. Feasibility of eradicating cerambycid larvae and pinewood nematodes infesting lumber with commerical 2.45 GHz microwave equipment. *Forest Prod. J.* 55(12):227–232.

Fleming, M. R., J. J. Janowiak, J. Kearns, J. E. Shield, R. Roy, D. K. Agrawal, L. S. Bauer, D. L. Miller, and K. Hoover. 2004. Parameters for scale-up of microwave treatment to eradicate cerambycid larvae infesting solid wood packing materials. *Forest Prod. J.* 54(7/8):80–84.

Food and Agriculture Organization of the United Nations (FAO). 2013. Draft revision of Annex 1: Approved treatments associated with wood packaging material to ISPM 15:2009 and consequential revision of Annex 2 (2006-011). Food and Agriculture Organization of the United Nations, Secretariat of the International Plant Protection Convention, Rome, Italy. https://www.ippc.int/en/publications/931, accessed April 6, 2024.

Gagnon, M. A., K. Hoover, K. K. Szymona, K. J. J. Janowiak, R. Mack, and M. Hamlin. 2019. Manufacturer update: Radio frequency dielectric heating for pallet sanitization. *Pallet Central Mag.* 19(6):30–32. https://www.palletcentral.com/page/PalletCentral_Mag., accessed May 1, 2024.

Henin, J. M., M. Leyman, A. Bauduin, B. Jourez, and J. Hébert. 2014. Phytosanitary treatment of European pallets by microwave: Developing a program to ensure compliance with ISPM 15 and monitoring its efficacy on the house longhorn beetle (*Hylotrupes bajulus* L.). *Eur. J. Wood Wood Prod*. 72:623–633.

Huntsberger, D. V. and P. Billingsley. 1987. Elements of Statistical Inference. 6th ed. Allyn & Bacon, Boston.

International Forestry Quarantine Research Group. 2012. Guidelines for the application and verification of dielectric heating as a phytosanitary measure. (Draft guidelines October 13, 2012) https://www.ippc.int/static/media/files/publications/en/2013/06/05/1347567272_2012_IFQRG-10-14_Draft_Dielectri.pdf, accessed Feb. 15, 2024.

Janowiak, J. J., K. K. Szymona, M. K. Dubey, R. Mack, and K. Hoover. 2022. Improved radio-frequency heating through application of wool insulation during phytosanitary treatment of wood packaging. *Forest Prods. J.* 72(2):1–7. https://doi.org/10.13073/FPJ-D-22-00009

Jiao, S. 2012. Development of non-chemical postharvest treatments for disinfecting agricultural products. PhD thesis. Washington State University, Pullman.

Kočí, V. 2019. Comparisons of environmental impacts between wood and plastic transport pallets. *Sci. Total Environ*. 686:514–528. https://doi.org/10.1016/j.scitotenv.2019.05.472

Laborelec, C. J. 2011. Application note on dielectric heating. https://www.slideshare.net/sustenergy/application-note-dielectric-heating, accessed July 14, 2023.

Mermelstein, N. H. 1997. Interest in radiofrequency heating heats up. *Food Technol*. 51(10):94–95.

Nelson, S. O. 1967. Chapter 3: Electromagnetic energy. *In*: Pest Control: Biology, Physical and Selected Chemical Methods. W.W. Kilgore and R.L. Doutt (Eds.). Academic Press, New York, pp. 89–146.

Olson, L. 2006. The economics of terrestrial invasive species: A review of the literature. *Agric. Resource Econ. Rev*. 35(1):178–194. https://doi.org/10.1017/S1068280500010145

Pimentel, D., R. Zuniga, and D. Morrison. 2005. Update on the environmental and economic costs associated with alien-invasive species in the United States. *Ecol. Econ*. 52(3):273–288. https://doi.org/10.1016/j.ecolecon.2004.10.002

Rattanadecho, P. 2004. Theoretical and experimental investigation of microwave thawing of frozen layer using a microwave oven (effects of layered configurations and layer thickness). *Int. J. Heat Mass Transf*. 47:937–945. https://doi.org/10.1016/j.ijheatmasstransfer.2003.08.019

Shottafer, J. E. and C. E. Shuler. 1974. Estimating heat consumption in kiln-drying lumber. Tech. Bull. 73, Life Science and Agricultural Experiment Station, University of Maine, Orono. 25 pp.

Szymona, K. and J. J. Janowiak. 2019. Commercial scale radio frequency phytosanitation of aspen pallet components; estimation of cost feasibility for the large-scale unit. Penn State Technical Report. Penn State University, University Park. 10 pp.

Szymona, K., J. J. Janowiak, K. Hoover, and R. Mack. 2020. Development of certification protocols and advancements for radio-frequency (rf) technology for phytosanitation of wood packaging material (WPM) in compliance with ISPM-15. International Forestry Quarantine Research Group (IFQRG-17), September 28–October 2, 2020, virtual meeting hosted by Penn State University, University Park.

Tubajika, K. M., J. J. Janowiak, R. Mack, and K. Hoover. 2007. Efficacy of radio frequency treatment and its potential for control of sapstain and wood decay fungi on red oak, poplar, and southern yellow pine wood species. *J Wood Sci*, 53(3):258–263.

United Nations Environment Programme (UNEP). 2000. The Montreal Protocol on Substances that Deplete the Ozone Layer. Secretariat for the Vienna Convention for the Protection of the Ozone Layer, March 2000. http://www.unep.org/ozone, accessed Sept. 9, 2024.

US Department of Energy. 2023. Total energy, monthly energy review, March 26, 2024. https://www.eia.gov/totalenergy/data/monthly/, accessed June 1, 2024.

Uzunovic, A., A. Dale, B. Gething, R. Mack, J. Janowiak, and K. Hoover. 2013. Lethal temperature for pinewood nematode, *Bursaphelenchus xylophilus,* in infested wood using radio frequency energy. *J. Wood Sci*. 59:160–170.

Weththasinghe, K. K., A. Akash, T. Harding, M. Subhani, and M. Wijayasundara. 2022. Carbon footprint of wood and plastic as packaging materials—An Australian case of pallets. *J Cleaner Prod.* 363:132446. https://doi.org/10.1016/j.jclepro.2022.132446